

Redshift distribution of Ly- α lines and metal systems

M. Demiański^{1,2}, A.G. Doroshkevich^{3,4}, & V.Turchaninov⁴

¹*Institute of Theoretical Physics, University of Warsaw, 00-681 Warsaw, Poland*

²*Department of Astronomy, Williams College, Williamstown, MA 01267, USA*

³*Theoretical Astrophysics Center, Juliane Maries Vej 30, DK-2100 Copenhagen Ø, Denmark*

⁴*Keldysh Institute of Applied Mathematics, Russian Academy of Sciences, 125047 Moscow, Russia*

Accepted ..., Received 1999 ... ; in original form 1999 ...

ABSTRACT

The observed redshift distribution of Ly- α lines and metal systems is examined in order to discriminate and to trace the evolution of structure elements observed in the galaxy distribution, at small redshifts, and to test the theoretical description of structure evolution. We show that the expected evolution of filamentary component of structure describes quite well the redshift distribution of metal systems and stronger Ly- α lines with $\log(N_{HI}) \geq 14$, at $z \leq 3$. The redshift distribution of weaker Ly- α lines can be attributed to the population of poorer structure elements (Zel'dovich pancakes), which were formed at high redshifts from the invisible DM and non luminous baryonic matter, and at lower redshifts they mainly merged and dispersed.

Key words: cosmology: large-scale structure of the Universe — quasars: absorption: general — surveys.

1 INTRODUCTION

During the last years an essential progress has been achieved both in the observations and interpretations of absorption spectra of quasars. Now a representative set of absorption lines with measured redshifts, column densities, and Doppler parameters is available and the main characteristics of absorbers and their evolution are, in general, established (see, e.g., Carswell 1995; Cristiani et al. 1995, 1996; Hu et al. 1995; Fernandez-Soto et al. 1996; Ulmer 1996; Cooke et al 1997; Dinshaw et al. 1995; Bahcall et al. 1993, 1996; Kim et al. 1997). The available information suggests various descriptions of absorbers ranging from pressure-confined gaseous clouds to associations with halos of galaxies (see discussions in Rees 1995; Charlton 1995; Fernandes-Soto et al. 1996; Miralda-Escude et al. 1996; Petitjean 1997). If at low redshifts a significant number of stronger Ly- α lines and metal systems are certainly associated with galaxies (Bergeron et al. 1992; Lanzetta et al. 1995; Cowie et al. 1995; Tytler et al. 1995; Le Brune et al. 1996) than the population of weaker absorbers, dominating at higher redshifts, has practically disappeared by the redshift $z \approx 2$ and only some weak Ly- α lines are observed far from galaxies even at small redshifts (Morris et al. 1993; Shull 1997).

Now the origin and evolution of absorbers are linked to the process of formation and evolution of high density structure elements (Petitjean et al. 1995; Miralda-Escude et al. 1996; Hernquist et al. 1996; Zhang et al. 1997, 1998; Theuns et al. 1998, 1999; Bryan et al. 1999; Davè et al. 1999;

Weinberg et al. 1998; Machacek et al. 2000). The numerical simulations of dynamical and thermal evolution of gaseous component use the same spectrum of initial perturbations that is responsible for the formation of DM and observed galaxy spatial distributions, and they successfully reproduce the main observed properties of absorbers. This allows us to consider the evolution of absorbers in a context of a more general process of nonlinear evolution of small initial perturbations of DM component and formation of observed galaxy distribution and to compare theoretical conclusions with observations.

This approach links the properties of absorbers, at high redshifts, with the spatial galaxy distribution at small redshifts and allows to trace some observational characteristics of nonlinear evolution of matter distribution up to redshifts $z \approx 3$.

The analysis of large modern redshift surveys such as the Durham/UKST Galaxy Redshift Survey (Ratcliffe et al., 1996) and the Las Campanas Redshift Survey (Shectman et al., 1996) demonstrates that the galaxy distribution in the universe can be roughly described as a joint network composed of galaxy filaments and walls. The analysis of both surveys shows that about 50% of galaxies are concentrated in wall-like elements surrounding huge underdense regions with a typical size of $50 - 100 h^{-1}$ Mpc ($h = H_0/100$ km/s/Mpc is the dimensionless Hubble parameter) (Doroshkevich et al. 1996, hereafter LCRS1; Doroshkevich et al. 2000). In many respects such elements are similar to the Great Wall (de Laparent, Geller & Huchra 1988; Ramella, Geller, & Huchra

1992). Galaxy filaments appear between walls and intertwine them into a joint structure. The hierarchy of poorer and sparser filaments – including single galaxies – can be considered as a bridge between the richer and poorer structure elements formed by the non luminous baryonic and dark matter (DM). Such poorer elements contain some fraction of hot gas and could be seen as Ly- α absorbers away from galaxies. Observations of weak Ly- α absorbers in voids, mentioned above, can be attributed to those poorer DM structure elements.

The evolution of structure elements formed by dark matter was investigated both theoretically, using the Zel'dovich theory (e.g., Zel'dovich 1970; Zel'dovich & Novikov 1983; Shandarin & Zel'dovich 1989), and numerically (e.g., Shandarin et al. 1995; Cole et al. 1997, 1998; Jenkins et al. 1998; Doroshkevich et al. 1999, hereafter DMRT; Demiański et al. 2000, hereafter DDMT). The statistical description of DM structure evolution for the CDM-like power spectra was given in Demiański & Doroshkevich (1999 hereafter DD99) and in DDMT. The main simulated characteristics of walls are found to be consistent with theoretical expectations.

Some progress in the theoretical interpretation of properties of absorbers has been recently achieved by Hui et al. (1997) and Nath (1997), who used the Zel'dovich approximation for a semi analytical description of some of the absorbers characteristics. Another considered theoretical approaches were based on the 'minihalo' model (Meiksin 1994), 'Cosmic Webb' theory (Bond & Wadsley 1997) and Press-Schechter method (Valageas et al. 1999).

In this paper we examine the observed redshift distribution of absorbers using the available information about the structure parameters at small redshifts (LCRS1; Doroshkevich et al. 2000; DMRT) and statistical description of DM structure evolution (DD99, DDMT) in models with CDM-like power spectra. We assume that the Lyman- α clouds trace the potential wells formed by DM pancakes, filaments and walls. This assumption was widely discussed earlier (Rees 1986; Ikeuchi & Ostriker 1986; Bond, Szalay & Silk 1988; Miralda-Escude & Rees 1993; Meiksin 1994; Hui et al. 1997; Nath 1997; Bond & Wadsley 1997; Valageas et al. 1999), and it is qualitatively consistent with results of numerical simulations (Petitjean et al. 1995; Hernquist et al. 1996; Petitjean 1997; Theuns et al. 1997; Davè et al. 1999; Weinberg et al. 1998).

The potential of this approach is limited due to the small number of observed absorbers and because the characteristics of structure derived from observations are not sufficiently accurately known. The theoretical description of DM structure evolution is also not complete. In particular, it cannot yet describe adequately the important process of disruption of structure elements and their transformation into a system of high density clumps. This process depends on many factors (Doroshkevich 1980; Vishniac 1983; Valinia et al. 1997) and strongly influences the observed properties of absorbers both at large and small redshifts (Miralda-Escude et al. 1996; DMRT; DDMT). Moreover, the evolution of DM structure elements and observed absorbers is not identical.

Nonetheless, even so limited information allows us to obtain a reasonable description and interpretation of some of the observed characteristics of absorbers. In this paper we consider the statistical description of redshift distribu-

tion of absorbers and metal systems which is more detailed, in some respects, than that usually used. The comparison of measured redshift distributions with approximate theoretical expectations (DD99) allows us to discriminate statistically the contributions of high density filamentary and lower density sheet-like structure elements formed by DM and gaseous components of matter, and to trace their evolution. These two components of structure elements can be roughly identified with two subpopulations of absorbers discussed, for example, in Bahcall et al. (1996) and Weymann et al. (1998).

This division of structure elements into filaments and more sheet-like walls and pancakes is inevitably statistical only. The more detailed analysis of DM and galaxy distribution, at small redshifts (DMRT, DDMT), demonstrates limitations of such description and shows that usually the morphology of structure elements can be more accurately characterized in terms of *degree of filamentarity and/or sheetness* only. The investigation of morphology and spatial distribution of DM and gaseous structure elements in simulations at high redshifts with the new powerful techniques (such as the Minimal Spanning Tree or Minkowski Functional), as well as direct comparison of morphological and other characteristics of the structure elements with their redshift distribution is required to clarify this problem and to obtain more detailed comparison of observed and simulated matter distributions.

This paper is organized as follows. The theoretical model of structure evolution and the technique necessary for the analysis are briefly described in Sec. 2. Sec. 3 contains information about the used observational databases. The results of statistical analysis are presented in Sec. 4. Discussion and conclusion can be found in Sec. 5.

2 REDSHIFT DISTRIBUTION OF ABSORBERS

2.1 Pancakes, filaments and walls associated with absorbers

The redshift distribution of absorbers can be characterized by the mean comoving free path between absorbers $\langle l \rangle$ (Sargent et al. 1980) as

$$dN(z) = \langle l \rangle^{-1} c(1+z)dt = \langle l \rangle^{-1} \frac{c |dz|}{H(z)} \quad (2.1)$$

$$H(z) = H_0 \sqrt{\Omega_m(1+z)^3 + (1-\Omega_m-\Omega_\Lambda)(1+z)^2 + \Omega_\Lambda}$$

where $dN(z)$ is the number of absorbers between z and $z+dz$, $\langle l \rangle^{-1}$ is the mean comoving linear number density of absorbers, c is the speed of light, Ω_m and Ω_Λ are correspondingly the dimensionless matter density and cosmological constant. The redshift dependence of the mean comoving linear number density of absorbers can be written as:

$$n_{abs} = \frac{c}{H_0} \langle l \rangle^{-1} = n_w(z) + n_f(z) + n_{pan}(z), \quad (2.2)$$

$$dN(z) = n_{abs} \frac{H_0 dz}{H(z)},$$

where the three terms in (2.2) correspond to three main types of structure elements observed at small redshifts: the

rich walls (n_w), filaments (n_f), formed by galaxies, and poor pancakes (n_{pan}), situated far from observed galaxies.

Such division of structure elements into three different subpopulations is made for the sake of simplicity only. In particular, there is an anisotropic sheet-like low density halo around all filaments, which in turn are later strongly disrupted into a system of high density clumps. The higher density ridges cross often the low mass pancakes. Walls are also often formed by a system of high density clumps and filaments connected by lower density bridges. This means that in nature, there is really only one population of structure elements with a broad variety of continually distributed properties, and these elements can be considered as the more typical and conspicuous ones. Nonetheless, the considered classification makes this analysis simpler and more transparent, as the rate of structure evolution depends upon the degree of filamentarity or sheetness.

2.2 Evolution of DM structure elements

In the DM dominated universe the basic characteristics of matter distribution are determined by the process of formation and evolution of DM structure elements. The observed characteristics of absorbers and parameters of DM structure elements are not identical but they are closely connected and relations between these parameters can emerge from suitable investigations.

For the CDM-like transfer function (Bardeen et al. 1986) and the Harrison-Zel'dovich initial power spectrum the approximate statistical description of the formation and evolution of DM structure elements based on the statistics of initial perturbations was obtained in DD99. The random formation and merging of Zel'dovich pancakes with 'mass' (column density of a pancake) m and their evolution, due to the transversal expansion or compression, are described by approximate expressions similar to the Press-Schechter relations. Similar approximate relations can be also written for the filamentary component of the structure. Here we will apply some of these results to describe the observed evolution of absorbers.

As is usual in the Zel'dovich theory the redshift dependence of all characteristics of structure is expressed through a function $B(\Omega_m, z)$, which describes the growth of perturbations in the linear theory. For the flat universe with $\Omega_m + \Omega_\Lambda = 1$, $\Omega_m \geq 0.1$, the function $B(z)$ can be approximated (DD99) with a precision better than 10% by the expression

$$B(z)^{-3} \approx \frac{1 - \Omega_m + 2.2\Omega_m(1+z)^3}{1 + 1.2\Omega_m}, \quad (2.3a)$$

and for an open universe with $0.1 \leq \Omega_m \leq 1$, $\Omega_\Lambda = 0$ as

$$B(z)^{-1} \approx 1 + \frac{2.5\Omega_m}{1 + 1.5\Omega_m} z \quad (2.3b)$$

(Zel'dovich & Novikov 1983). For $\Omega_m = 1$, $\Omega_\Lambda = 0$ both expressions give $B^{-1}(z) = 1 + z$.

2.2.1 Formation and evolution of DM structure

The evolution of DM structure can be outlined as a progressive matter concentration within more and more massive structure elements which can be roughly discriminated into

pancakes, filaments and walls. The structure elements are primarily formed as Zel'dovich pancakes (Shandarin et al. 1995), but later are successively transformed into filaments and/or (elliptical) clouds. At high redshifts $z \geq 5 - 7$ a significant fraction of matter ($\sim 80\%$) can be compressed into low mass pancakes with $M_{cl} \sim 10^7 - 10^9 M_\odot$. Later some of such clouds can evolve into dwarf galaxies, some could disperse, but the main fraction will be accumulated by more massive structure elements. Properties of the surviving and relaxed clouds can be similar to those discussed in the 'mini-halo' model (Rees 1986, 1995; Miralda-Escude & Rees 1993; Meiksin 1994)

The filamentary component of structure also forms at high redshifts due to the compression of some part of pancakes, and, at $z \sim 1 - 3$, it is, probably, the most conspicuous population of high overdensity structure elements accumulating 40 – 50% of DM particles (see., e.g., Governato et al. 1998, Jenkins et al. 1998). Further evolution of structure can be described as a successive merging of lower mass pancakes and filaments into more and more massive wall-like structure elements. The largest observed wall-like elements, similar to the Great Wall, are formed at redshifts $z \leq 1$ due to the infall and intermixture of smaller pancakes and filaments.

In observations, at $z \leq 1$, galaxy filaments are usually situated within extended under dense regions surrounded by higher density walls, and they form an irregular broken network. This network can be described as a trunk, that is the longest filament of the complex, and a set of shorter branches. This means that the spatial distribution of filaments can be conveniently characterized by the mean 2D surface number density, $\sigma_f(z)$, that is the mean number of filaments intersecting a unit area of arbitrary orientation. For observed galaxy filaments it is estimated as $\sigma_f(0) \approx (1 - 0.7) \cdot 10^{-2} h^2 \text{Mpc}^{-2}$ (LCRS1). The spatial distribution of observed walls can be characterized by their mean separation $\langle D_w \rangle$ and by their linear density, σ_w , that is the mean number of walls intersecting a unit length of a random straight line. For the observed galaxy walls it is estimated as $\langle D_w \rangle \approx 40 - 60 h^{-1} \text{Mpc}$ that corresponds to $\sigma_w \approx 2.5 - 1.6 \cdot 10^{-2} h \text{Mpc}^{-1}$. The low mass pancakes can be considered as isolated objects and characterized by the mean 3D number density $\nu_{pan}(z)$.

Simulations show that rich pancakes and filaments are relaxed (at least along shorter axes) and are surrounded by an extended DM (and gaseous) halo. Central parts of dense elements are gravitationally confined and are unstable with respect to the small scale disruption (DDMT). Some of the high density clumps are usually embedded in filaments and walls what essentially accelerates the relaxation of compressed matter. In observations, effects of such disruptions are seen as groups and clusters of galaxies.

The basic properties of DM structure elements vary in a broad range, but it can be expected that galaxies are formed mainly within richer high density filaments and pancakes. The essential fraction of poor pancakes and, perhaps, filaments, can be invisible, as it does not contain sufficiently bright galaxies. Such structure elements can be observed as weak Ly- α absorbers situated far from any galaxy. Some number of such absorbers situated at a distance of up to $5 h^{-1} \text{Mpc}$ from the closest galaxy was found by Morris et al. (1993) and Shull (1997).

This description agrees well with results of numerical

simulations at small redshifts (DDMT). The validity of this description, when it is applied to structure at high redshifts, is not yet reliably verified with available simulations due to a small density contrast of poor structure elements. The first tests show, however, the existence of three kinds of structure elements, namely, high density filaments and clumps, and low density pancakes in DM spatial distribution at $z = 3$. The theoretical description (DD99) confirms also the self-similar character of structure evolution (at least when the Zel'dovich approximation can be applied). This picture is also qualitatively consistent with other simulations of structure evolution (Miralda-Escude et al. 1996; Governato et al. 1998; Jenkins et al. 1998; Meiksin 1998; DMRT; Davè et al. 1999; Weinberg et al. 1998).

2.2.2 Main factors of structure evolution

The four main factors characterizing the structure evolution are

- (i) successive formation of structure elements with larger and larger masses,
- (ii) merging of earlier formed, more numerous, low mass filaments and pancakes
- (iii) expansion or compression of matter along filaments and pancakes
- (iv) small scale clustering of compressed matter and disruption of structure elements.

The action of these factors was discussed in DD99 (Secs. 4.1, 4.2 & 5.2) and it was shown that for the CDM-like initial power spectrum and Gaussian initial perturbations it can be approximately described by simple analytical expressions. Some of these relations were tested and confirmed through the direct comparison with DM simulations (DDMT). Here we will briefly summarize these results.

The distribution function of Zel'dovich pancakes with mass (surface density) m_p , $N_p(m_p)$, can be written as follows:

$$N_p(m_p) \propto \frac{1}{\sqrt{m_p \langle m_p \rangle}} \exp\left(-\frac{m_p}{\langle m_p \rangle}\right) \operatorname{erf}\left[\sqrt{\frac{m_p}{\langle m_p \rangle}}\right], \quad (2.4)$$

$$\langle m_p \rangle \propto B^2,$$

where the successive merging of low mass pancakes in the course of formation of richer pancakes is described by the erf -function. The process of merging decreases the number density of numerous low mass structure elements – both filaments and pancakes – with $m_p \ll \langle m_p \rangle$, but its influence becomes negligible for rare, massive, wall-like structure elements, with $m_p \geq \langle m_p \rangle$, and rare rich filaments. For the fraction of pancakes with $m_{min} \leq m_p \leq m_{max}$ from (2.4) we have:

$$f_p \propto \operatorname{erf}^2\left[\sqrt{\frac{m_{max}}{\langle m_p \rangle}}\right] - \operatorname{erf}^2\left[\sqrt{\frac{m_{min}}{\langle m_p \rangle}}\right]. \quad (2.5)$$

For rich walls formed presumably at $z \leq 1 - 1.5$ with $m_{max} \rightarrow \infty$ and $m_{min} \equiv m_w \sim \langle m_p \rangle$ this relation is simplified and approximately we have

$$f_w \propto 1 - \operatorname{erf}^2\left[\sqrt{\frac{m_w}{\langle m_p \rangle}}\right] \propto \operatorname{erfc}\left[\sqrt{\frac{m_w}{\langle m_p \rangle}}\right], \quad (2.6)$$

what constrains the population of massive pancakes. For the subpopulation of poor pancakes similar relation

$$f_w \propto 1 - \operatorname{erf}^2\left[\sqrt{\frac{m_{min}}{\langle m_p \rangle}}\right] \propto \exp\left[-\frac{m_{min}}{\langle m_p \rangle}\right],$$

is valid only at higher redshifts $z \geq 3.5 - 4$, when $m_{max} \gg m_{min} \sim \langle m_p \rangle$, whereas during the most interesting period, $z \leq 3.5$, when $m_{min} \ll \langle m_p \rangle$, the second term in (2.5) can be omitted.

The discrimination of rich walls and poor pancakes seems to be artificial, in some respects, but it allows us to provide a closer connection with observed galaxy and simulated DM distributions at smaller redshifts. Moreover, rich walls are certainly strongly nonhomogeneous and disrupted into high density clumps and filaments, what essentially decreases their covering factor. Due to these peculiarities such walls can form a special class of objects.

The distribution function of filaments with mass (linear density) m_f is found to be proportional to

$$N_f \propto \frac{1}{\langle m_f \rangle} K_0^2\left(\sqrt{\frac{m_f}{4\langle m_f \rangle}}\right), \quad \langle m_f \rangle \propto B^4, \quad (2.7)$$

where $K_0(x)$ is the modified Bessel function (DD99) and the fraction of rich filaments, with $m_f \geq \langle m_f \rangle$, is

$$f_f \propto \exp\left(-\sqrt{\frac{m_f}{\langle m_f \rangle}}\right). \quad (2.8)$$

As before, the infall of filaments into rich walls decreases the fraction of filaments associated with the network $\propto \operatorname{erf}[\sqrt{m_p/\langle m_p \rangle}] \propto B^{-1}$.

Furthermore, the properties of structure are essentially changed due to matter expansion and/or compression in transversal directions. Compression results in transformation of pancakes into filaments and high density clouds, what decreases their effective surface and, also, the probability to see such a structure element as an absorber. Strong expansion increases the surface of pancakes and the length of filaments and correspondingly decreases their density. In the limiting case, low mass pancakes and filaments can be transformed into a system of high density clumps or they can even completely disperse. The expansion decreases also the column density of HI below the observational threshold, $N_{HI}^{(thr)} \approx 10^{12} \text{ cm}^{-2}$, what makes such elements invisible as absorbers. Therefore, the population of structure elements identified with absorbers is restricted by the condition of their relatively slow expansion or compression in transversal directions. Fraction of such low mass pancakes decreases with time $\propto \operatorname{erf}^2[\sqrt{m_p/\langle m_p \rangle}]$, and fraction of such low mass filaments decreases $\propto \operatorname{erf}[\sqrt{m_p/\langle m_p \rangle}] \propto B^{-1}$. The influence of these factors is less important for rare rich walls and filaments.

Due to gravitational instability of compressed matter both pancakes and filaments are usually disrupted into a system of high density clouds linked by low density bridges. Such disruption occurs more rapidly in the central high density parts of structure elements, but, probably, its impact is not so important for the extended lower density halo. When these processes are taken into account the final relations become very cumbersome and therefore such more detailed treatment is not really justified for when only limited set of observed absorbers is available.

When these factors are taken into account we can only approximately describe the expected evolution of walls, filaments, and low mass pancakes associated with the absorbers. The comoving linear number density of massive walls, $\sigma_w(m)$ with $m \geq m_w$, the comoving surface number density of filaments, $\sigma_f(m)$, and the comoving number density of pancakes, $\nu_{pan}(m)$, can be approximated by simple expressions:

$$\sigma_w \propto \exp\left(-\frac{b_w(m)}{B^2}\right), \quad (2.9)$$

$$\sigma_f \propto B^{-2} \exp\left(-\frac{b_f(m)}{B^2}\right), \quad (2.10)$$

$$\nu_{pan} \propto \text{erf}^2\left(\frac{b_1}{B}\right) \left[\text{erf}^2\left(\frac{b_2}{B}\right) - \text{erf}^2\left(\frac{b_3}{B}\right) \right], \quad (2.11)$$

where the parameters b_w , b_f & $b_3(m)$ and the exponential terms in (2.9) and (2.10) restrict formation of structure elements with masses $> m$, the term B^{-2} in (2.10) describes successive infall of filaments into richer walls and the decrease, due to expansion or compression, of number of filaments observed as absorbers with $N_{HI} \geq N_{HI}^{(thr)}$. The decrease of the number density of pancakes is described by the factor b_1 in (2.10).

For restricted redshift interval $z \leq 3.5$ the three parameter expression for ν_{pan} can be approximated by a simpler one parameter expression

$$\nu_{pan} \propto B^{-3} \exp\left(-\frac{b_{pan}(m)}{B^2}\right), \quad (2.12)$$

which correctly describes the asymptotical behavior of ν_{pan} at small and large redshifts. In the intermediate region it provides a reasonable precision $\sim 10 - 15\%$, for $z \leq 3.5$. The more complicated relation (2.11) provides better description of absorbers evolution especially at higher redshifts $z \geq 3 - 3.5$ and can be used for more refined fits.

High density clouds and galaxies are usually embedded in filaments and pancakes and cannot be distinguished as a special class of absorbers. These problems were discussed with more details in our other publications DD99, DMRT and DDMT.

2.3 Model of absorbers evolution

The relations (2.3), (2.9) - (2.12) cannot give the full description of observed redshift distribution of absorbers, but they suggest possible redshift evolution of various types of absorbers and introduce the function $B(z, \Omega_m)$ as an important characteristic of such evolution. It is important that the redshift evolution of free-path between walls, filaments, and low mass pancakes is expected to be different, and therefore, it might be possible to single out statistically these three subpopulations of absorbers, and to establish correlations between the evolutionary rates and other observational characteristics of absorbers.

The DM structure is quite complicated in itself as it is composed of several types of structure elements with different evolutionary histories. Furthermore, properties and evolution of the observed gaseous and DM structure elements are not identical, because of the influence of additional factors on the evolution of gaseous component of DM

confined structure elements and, therefore, even more complicated evolution of absorbers can be expected. The action of these factors usually decelerates the evolution of gaseous component but, due to very small density of this component, its impact on the evolution of DM component is negligible. Thus, the formation of weak absorbers within "minivoids" does not accompanied by the formation any DM structure elements (Bi & Davidsen 1997; Zhang et al. 1998; Davé et al. 1999).

The observational restrictions such as the condition $N_{HI} \geq N_{HI}^{(thr)}$ constrain also the population of absorbers and the observed evolution of absorbers. Thus, for example, the exponential growth of fraction of massive high temperature pancakes (in the limiting case, walls similar to the Great Wall) is not found in the observed distribution of absorbers (Sec. 4). Moreover, the mean measured b - parameter of absorbers, related to the gas temperature, remains constant for the observed redshifts $2.5 \leq z \leq 3.3$. This means that, possibly, some rich DM structure elements are not yet identified in the absorption spectra of quasars.

The redshift dependence of n_{abs} is driven both by the evolution of spatial characteristics of DM structure elements, discussed above, and by evolution of their covering factor, which characterizes the probability of formation of absorption line at the intersection of line of sight and a structure element. The covering factor depends on local conditions such as, for example, variations of the UV background and activity of nearest galaxies. Now it can be also described phenomenologically.

The important role of UV background is well established after the discussion in Sargent et al. (1980), but the UV intensity and its possible variation with redshift is known only with large uncertainty (see, e.g., Haardt & Madau 1996; Cook, Espey & Carswell 1997). The influence of systematic variations of UV radiation is more important at small ($z \leq 2$) and higher ($z \geq 3 - 3.5$) redshifts where the statistic of absorbers is strongly limited. At intermediate redshifts $2.5 \leq z \leq 3.5$ where the main fraction of observed absorbers is situated the systematic variations of UV radiation are not so strong, but this radiation is probably responsible for the significant irregular variations of absorbers density.

The redshift distribution of observed absorbers can be distorted by the formation of artificial caustics in the redshift space (McGill 1990; Levshakov & Kegel 1996, 1997). As was shown in DDMT the impact of this effect is certainly small at small redshifts. At intermediate redshifts and for the usually used CDM-like power spectra the formation of artificial caustics is partly suppressed due to strong matter concentration within low mass structure elements discussed in DD99 and Zhang et al. (1998). This factor transforms the continuous matter infall into pancakes to discontinuous one, increases the density gradient near pancake boundaries and partly prevents the formation of artificial caustics. Moreover, such an artificial caustic is actually the preliminary stage of formation of a real caustic, and, so, it is rapidly transformed into a real one. This factor can moderately change the discussed redshift dependence of absorbers.

The contribution of artificial caustics and absorbers within "minivoids" as well as of short-lived rapidly expanding or contracting pancakes is more important at higher redshifts, when weak absorbers dominate. These factors gener-

ate an essential noise what is usually typical for the period preceding the epoch of regular evolution. At such redshifts, the available statistics of observed absorbers is very poor, and our analysis becomes unreliable. Perhaps, more detailed and careful investigations based upon the simulations will allow to discriminate observationally between this noise and long-lived structure elements (see, e.g., discussion in Zhang et al. 1998) that will essentially improve and simplify the comparison with theoretical expectations.

The more detailed description of structure evolution significantly increases the number of fit parameters for limited available statistics of observed absorbers, and more detailed description accompanied by a further growth of number of fit parameters does not seem to be justified. Hence, as the first step, we will fit the observed redshift distribution of absorbers to relations similar to theoretically expected expressions (2.9)–(2.12), but instead of the functions $b(m)$, arbitrary fitting parameters will be used. The difference between the observed and expected redshift distributions can be attributed to the influence of omitted factors. Similar analysis can be repeated with richer data base and/or with available numerical simulations.

2.3.1 Absorption in wall-like elements

The first term in (2.2), n_w , describes absorption associated with wall-like elements. Now these elements accumulate $\approx 50\%$ of galaxies and their possible contribution cannot be rejected *a priori*. The observed mean separation of walls is about $40 - 60 h^{-1}\text{Mpc}$ and the comoving linear number density of such elements is $\sigma_w(0) \approx 2.5 - 1.5 \cdot 10^{-2} h\text{Mpc}^{-1}$ (LCRS1). These elements are formed during late evolutionary stages and can be observed, primarily, at small redshifts, $z \leq 1 - 1.5$.

Taking into account expressions (2.3) & (2.9) we will approximate the mean dimensionless linear number density of absorbers associated with such elements by the two parameter function

$$n_w(z) \approx \kappa_w E(c_w, z), \quad (2.13)$$

$$\kappa_w = \frac{c\sigma_w(0)\alpha_w}{H_0}, \quad E(c_w, z) = \exp[-c_w(B^{-2}(z) - 1)],$$

where the covering factor $\alpha_w < 1$, and the parameter c_w characterize probability of formation of an absorption line in a wall and the period of wall formation, respectively. The observed wall-like structure elements are strongly disrupted (see, e.g., Fig 5 in Ramella et al. 1992) and therefore we can expect that $\alpha_w \ll 1$, $n_w(0) = \kappa_w \approx 60\alpha_w$.

2.3.2 Absorption in filamentary elements

The second term in (2.2), n_f , describes absorption in filaments formed by DM, galaxies and intergalactic gas. The filamentary component of the structure accumulates $\approx 50\%$ of DM and galaxies and forms a joint network of structure between wall-like elements. As was noted above, the mean observed 2D surface density of galaxy filaments is estimated as $\sigma_f(0) \approx 0.01 h^2 \text{Mpc}^{-2}$.

The mean free-path between filaments depends on their surface density, σ_f , and their diameters. To find it we consider the intersection of cylindrical filaments with typical

radius of gaseous halo R_f and a random cylindrical core with radius r and length L . The mean number of such intersections can be found with standard methods (Kendall & Moran 1963, Buryak et al. 1994) as follows:

$$\langle N_{int} \rangle = \pi\sigma_f L(r + R_f).$$

The mean free-path between such cylindrical filaments along a line of sight can be approximated by

$$\langle l_f \rangle \approx L/\langle N_{int} \rangle|_{r=0} = (\pi\sigma_f R_f)^{-1}, \quad (2.14)$$

while the mean length of a line of sight within a filament is $\approx 2R_f$.

Taking into account expressions (2.10) we will approximate the mean dimensionless linear number density of absorbers associated with filaments by a two parameter function

$$n_f(z) \approx \kappa_f(1 + z)B^{-2}(z)E(c_f, z) \quad (2.15)$$

$$\kappa_f = \frac{c}{H_0}\pi R_{eff}\sigma_f(0), \quad E(c_f, z) = \exp[-c_f(B^{-2}(z) - 1)],$$

$$R_{eff} = \alpha_f \langle R_f \rangle = \frac{\kappa_f H_0}{\pi c \sigma_f} \approx 10.6 \kappa_f \left(\frac{\sigma_f}{0.01 h^2 \text{Mpc}^{-2}} \right) h^{-1} \text{kpc}.$$

Here $\langle R_f \rangle$ is the mean radius of gaseous halo of a filament, the covering factor $\alpha_f(z) < 1$ characterizes the probability of formation of an absorption line within a separate filament, and the factors $1 + z$, and $B^{-2}(z)$, describe the expected variation of surface density of absorbers associated with filaments due to the general expansion of the universe, merging, and expansion or compression of filaments. The parameter c_f characterizes the period of formation of the main fraction of observed filaments.

The mean radius of gaseous halo of filaments, $\langle R_f \rangle$, can vary with the redshift and along the filament, because the observed galactic density varies along the filament as well. This means that our statistical estimate of averaged $\langle R_f \rangle$ is weighted by the matter distribution along filaments at different redshifts.

More detailed models of absorbers associated with DM filaments can be developed. They depend however on many parameters which cannot be adequately determined from the available database. Hence, in this paper we will restrict our consideration to the two parametric model discussed above.

2.3.3 Absorption in low mass structure elements

The third term in (2.2), n_{pan} , describes absorption by low mass structure elements. The available information about properties of this population at small redshifts is very limited and we can estimate only the mean linear number density of such pancakes $n_{pan}(0) = \kappa_{pan}$. Taking into account expressions (2.12), we will approximate the mean dimensionless linear density of such absorbers, as

$$n_{pan}(z) \approx \kappa_{pan}(1 + z)^2 B^{-3}(z)E(c_{pan}, z), \quad (2.16)$$

$$E(c_{pan}, z) = \exp[-c_{pan}(B^{-2}(z) - 1)].$$

Here the factors $(1 + z)^2$, and $B^{-3}(z)$, describe the expected variation of the density $n_{pan}(z)$, caused by the general expansion, merging of pancakes, and their compression, and/or

expansion in transversal directions. The parameter κ_{pan} is the effective dimensionless free-path between such absorbers at $z = 0$, and c_{pan} characterizes the period of formation of the main fraction of observed pancakes with $N_{HI} \geq N_{HI}^{(thr)}$.

The expressions (2.13), (2.15) & (2.16) give probable fitting relations to the observed evolution of absorbers associated with various types of structure elements. They allow us to estimate, in principle, the effective radius of gaseous component of filaments and the parameters of cosmological model Ω_m and Ω_Λ . All fitting parameters have clear interpretation.

Here we do not consider the possible contribution of any high density clouds, because they are usually embedded in DM filaments and pancakes. This contribution is small, at least at redshifts $z \leq 3$, and cannot be reliably singled out with available database, but it probably is more important at higher redshifts.

2.4 Observed linear number density of structure elements

The small scale clustering of absorption lines has been reported in many papers (see, e.g., Cristiani et al. 1995, 1996; Ulmer 1996), and it is especially important for metal systems. It implies that a complex of nearby lines can be generated in the same structure element. As we are interested in statistics of structure elements this factor must be taken into account. To do this we will use a technique developed earlier for the core-sampling method (Buryak et al. 1994; LCRS1), which allows us to select a Poisson-like subsample of points from a general sample. The redshift dependence of the mean number density of the subsample characterizes the redshift evolution of uncorrelated absorbers, which can be identified with separate structure elements.

This method uses separation of neighboring lines rather than the lines redshift itself, what attenuates somewhat the influence of selection effects inherent in individual spectra. If the number of lines in a sample is $\geq 30 - 50$ we can estimate the parameters of Poisson distribution with a reasonable precision $\approx 10 - 20\%$. Hence, we can use the available catalogues, what is important for the metal systems, as number of such systems in individual absorption spectra is usually small.

The major points of the method can be summarized as follows:

(i) Separation between lines is characterized by the dimensionless comoving distance

$$\Delta l = H_0 \Delta z / H(z). \quad (2.17)$$

(ii) A subsample of lines, in an interval $z - dz < z < z + dz$, taken from all spectra under investigation is organized into an ‘equivalent single field’ by combining the line separations Δl one after the other along a line.

(iii) Distribution of absorbers obtained in that way is assumed to be Poissonian for larger separations. 1D cluster analysis is used to discriminate the Poisson-like subsample among the sample of points, and to find the number, and the mean linear number density of such points. The theoretical groundwork for such an approach was developed by Buryak, Demiański, & Doroshkevich (1991).

Using the standard 1D clustering analysis, the mean

number of Poisson points in the sample, N_P , and their mean linear number density, n_P , are found by the maximum likelihood fit to the relation

$$\ln(N_l) = \ln(N_P) - n_P R_l, \quad (2.18)$$

where R_l and N_l are the variable linking length and the related number of clusters, respectively. Note that for a truly Poisson sample parameters N_P & n_P are related to the length of the ‘equivalent single field’, D_0 , defined by the first and the farthest point by

$$D_0/N_P = n_P. \quad (2.19)$$

Thus, the difference between the values N_P and n_p obtained from equation (2.18) and from equation (2.19), and variations of the actual number of clusters along a straight line (2.18) give us a measure of error made due to the difference of the actual from the assumed (Poisson) distribution for absorbers along the line of sight. To decrease this error we use an automatic procedure, which finds the optimal range of R_l for the fit to equation (2.18). Both upper and lower limits of R_l were varied to obtain the best fit for the linear number density of absorbers $n_{abs}(z)$.

As a rule, the precision of this method increases with the number of lines, $N_{line}(z)$, in the interval $z - dz < z < z + dz$. For $N_{line}(z) > 50$, any random variation does not exceed 10%, and the real error is defined by the systematic variations of the sample under investigation. For smaller $N_{line}(z)$, random variations become essential. This condition restricts the choice of optimal interval to $dz \approx 0.2 - 0.25$.

3 THE DATABASE

The present analysis is based on spectra available in the literature. The list of such objects is given in Table 1.

The distribution of lines over redshift is nonhomogeneous and majority of lines are concentrated at $z \approx 3$. Using the technique described above, we can obtain the linear density of Poisson subsample of absorbers, at $z \leq 3.2$, with a reasonable precision of about of 10 – 20%. Distribution of absorbers, at $z \geq 3.2$, is based primarily on the 430 lines of QSO 0000-260 (Lu et al. 1996), and here the statistics of lines is rather poor. Inclusion of the spectrum of QSO 1033-033 extends the redshift interval up to $z \approx 4.4$, but it cannot improve inadequate representativity of the sample at $z \geq 3.2$. Samples of poorer lines, with $\log N_{HI} \leq 13$, are incomplete at all redshifts.

A few samples of observed metal systems were analyzed. Here we present results obtained for the richest recent sample (Vanden Berk et al. 1999). This catalogue contains 901 separations between lines of neighboring metal systems from 237 spectra of quasars at redshifts $0 \leq z \leq 3.5$.

The published Ly- α lines with different N_{HI} were organized into six samples listed in Table 2. All samples were supplemented by the HST data (Bahcall et al. 1993, 1996; Jannuzzi et al. 1998). The samples with $N_{HI} \geq 13.8$, are associated mainly with the filamentary component of the structure, whereas samples with $N_{HI} \geq 13$, and $N_{HI} \geq 12$, are associated predominantly with the poor pancakes.

Table 1. QSO spectra from the literature

Name	z_{em}	z_{min}	z_{max}	FWHM km/s	No of lines
1331 + 170 ¹	2.10	1.7	2.1	18	69
1101 – 264 ²	2.15	1.8	2.1	9	84
1225 + 317 ³	2.20	1.7	2.2	18	159
1946 + 766 ⁴	3.02	2.4	3.0	8	461
0636 + 680 ⁵	3.17	2.5	3.0	8	313
0302 – 003 ⁵	3.29	2.6	3.1	8	266
0956 + 122 ⁵	3.30	2.6	3.1	8	256
0014 + 813 ⁵	3.41	2.7	3.2	8	262
0000 – 260 ⁶	4.11	3.4	4.1	7	431
2126 – 158 ⁷	3.26	2.9	3.2	11	130
0055 – 259 ⁸	3.66	2.9	3.1	14	313
1700 + 642 ⁹	2.72	2.1	2.7	15	85
2206 – 199 ¹⁰	2.56	2.1	2.6	11	101
1033 – 033 ¹¹	4.50	3.7	4.4	18	299

1. Kulkarni et al. (1996), 2. Carswell et al. (1991), 3. Khare et al. (1997), 4. Kirkman & Tytler (1997), 5. Hu et al., (1995), 6. Lu et al. (1996), 7. Giallongo et al. (1993), 8. Cristiani et al. (1995), 9. Rodriguez et al. (1995), 10. Rauch et al. (1993), 11. Williger et al. (1994),

Table 2. Samples of absorbers.

sample	N_{QSO}	$\log N_{HI}$	N_{lines}	N_{lines}^{HST}	W_{HST}
Q_{14}^{14}	14	14	686	590	0.5
Q_{14}^{138}	14	13.8	971	590	0.5
Q_{14}^{13}	14	13.0	2351	933	0.25
Q_{12}^{13}	12	13.0	1986	933	0.25
Q_{12}^{12}	14	12.0	3177	1000	0.
Q_{12}^{12}	12	12.0	2780	1000	0.

4 STATISTICAL ANALYSIS OF STRUCTURE EVOLUTION

In this section the main results are presented for the redshift distribution of both Ly- α lines and metal systems. They confirm that the redshift distribution of Ly- α lines is a superposition of several populations, with different evolutionary histories (Bahcall et al. 1996). Using the method and the fitting relations discussed in Sec. 2 for the analysis of samples with different N_{HI} , we can roughly discriminate two populations of absorbers, and describe their evolution. Our estimates use essentially the HST data for $z \leq 1.5$.

For three cosmological models the distribution of absorbers was fitted to the expression

$$n_{abs} = \frac{\kappa_f(1+z)}{B^2(z)} E(c_f, z) + \frac{\kappa_{pan}(1+z)^2}{B^3(z)} E(c_{pan}, z) \quad (4.1)$$

$$E(c, z) = \exp[-c \cdot (B^{-2}(z) - 1)].$$

The function $B(z)$ was introduced in (2.3). The main results are plotted in Figs. 1 – 5, and the best fit parameters, κ_f , c_f , κ_{pan} , and

$$R_{eff} = \frac{\kappa_f H_0}{\pi c \sigma_f} \approx 10.6 \kappa_f \left(\frac{\sigma_f}{0.01 h^2 \text{Mpc}^{-2}} \right) h^{-1} \text{kpc}, \quad (4.2)$$

are listed in Tables 3 – 5. For samples of richer absorbers $c_{pan}=0$, whereas for samples of poorer absorbers $c_{pan} \approx 0.05 \pm 0.05$ was found with large errors and, so, it is omitted in Table 4.

Table 3. Fit parameters for the filamentary component at $z \leq 3$.

Ω_m	Ω_Λ	R_{eff}^{met} $h^{-1} \text{kpc}$	c_f^{met}	R_{eff}^{HI} $h^{-1} \text{kpc}$
1.0	0	40 ± 1.5	0.07 ± 0.03	98 ± 2.4
0.5	0	52 ± 1.6	0.15 ± 0.04	118 ± 3.3
0.3	0.7	38 ± 1.7	0.13 ± 0.04	69 ± 3.5

4.1 The redshift distribution of metal system and stronger HI lines

It can be expected that the redshift distribution of metal systems and stronger Ly- α lines is connected with the evolution of richer structure elements, which are seen in galaxy surveys as filaments and walls. To examine this hypothesis the function $n_{abs}(z)$ was found for the sample of metal systems, and the samples of strongest Ly- α lines Q_{14}^{14} , and Q_{14}^{138} . The analysis shows that in all cases no more than 10 – 15% of all lines can be attributed to the massive wall-like elements, what is consistent with the large separation of walls ($\geq 50 h^{-1} \text{Mpc}$) and their strong disruption into a system of high density clouds, what decreases their covering factor.

For all considered cosmological models the redshift distributions of Ly- α absorbers, for samples Q_{14}^{14} , and Q_{14}^{138} , are well fitted, at $z \leq 3$, to the one parameter function (4.1) with $c_f = 0$, and $\kappa_{pan} = 0$. The redshift distribution of metal systems is well fitted to the two parameter function (4.1) with $\kappa_{pan} = 0$. The best parameters of these fits are listed in Table 3. They show that metal systems are predominantly formed within inner regions of gaseous halos of filaments, whose size, R_{eff}^{met} , is about half the size of hydrogen halos, R_{eff}^{HI} . Both sizes are consistent with those observed directly at small z : $R_{HI} \sim 100 – 150 h^{-1} \text{kpc}$ (Lanzetta et al. 1995), and $R_{met} \sim 40 – 50 h^{-1} \text{kpc}$ (see, e.g., Le Brune et al. 1996), and to the expected size of DM halo (Bahcall et al. 1996). The precision of estimates of R_{eff} depends on the representativity of the sample used.

These results suggest that the redshift distribution, and the column density of absorbers are strongly correlated, and corroborate the identification of strong HI absorbers, and metal systems, with the filamentary component of the structure of the universe. They show that such filaments were probably formed at redshifts $z \geq 2$, but their enrichment by metals could occur later, at redshifts $z \approx 2$ and smaller.

At redshifts $z \geq 3$, the situation becomes more complicated, and the observed absorber distribution is no longer described by the one parameter fit plotted in Fig. 2 by dotted lines. To obtain a reasonable description, even for the redshift distribution of stronger absorbers, at $z \geq 3$, the three parameter fit (4.1) with $c_{pan} = 0$ must be used. This indicates that at $z \geq 3$ progressively increasing part of stronger absorbers must be assigned to pancakes.

The best parameters of these fits are listed in Table 4, and fitting functions $n_{abs}(z)$ are plotted in Fig. 2 by solid and long dashed lines. These estimates of c_f and R_{eff} crucially depend on the region of redshifts $2.5 \leq z \leq 3.3$, and could be sensitive to the possible evolution of filaments. They show that the formation of such filaments described by the exponential term in (4.1) could occur at redshifts $z \geq 1$, while later the surface density of filaments progressively decreases. The effective radii listed in Table 4 exceed by about 2 – 3 times those listed in Table 3 for smaller redshifts.

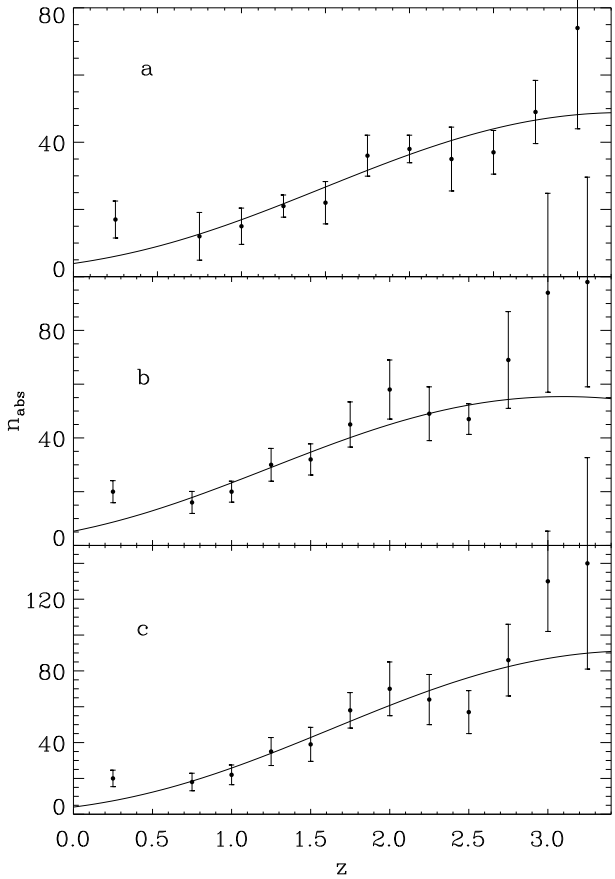


Figure 1. n_{abs} vs. z for metal systems for cosmological models with $\Omega_m = 0.3$, $\Omega_\Lambda = 0.7$ (a), $\Omega_m = 0.5$, $\Omega_\Lambda = 0$ (b), and $\Omega_m = 1$ (c).

This fact can be attributed to the progressive compression, small scale disruption, and relaxation of dark matter within and around filaments, which is accompanied by the progressive dissipation of gaseous halo of filaments. The observed evolution can also be partly assigned to the variations of background UV radiation with redshift.

At redshifts $z \geq 2 - 2.5$, more and more essential fraction of strong absorbers is associated with rich pancakes, and, at $z \geq 3.5$, the pancakes become dominant, even for this population. This fact probably indicates the period of more rapid transformation of rich pancakes into filaments.

This conclusion is based on poor statistics of absorbers, at $z \geq 3$, and should be tested with more representative sample of absorbers and with simulations.

For our samples the parameters of standard fit to

$$dN/dz = N_0(1+z)^{\gamma_z}, \quad (4.3)$$

are:

$$N_0^{met} = 6.8 \pm 0.5, \quad \gamma_z^{met} = 0.35 \pm 0.25, \quad (4.4)$$

$$N_0^{HI} = 12.7 \pm 2, \quad \gamma_z^{HI} = 1.5 \pm 0.3, \quad (4.4)$$

with a weak dependence on the considered cosmological models.

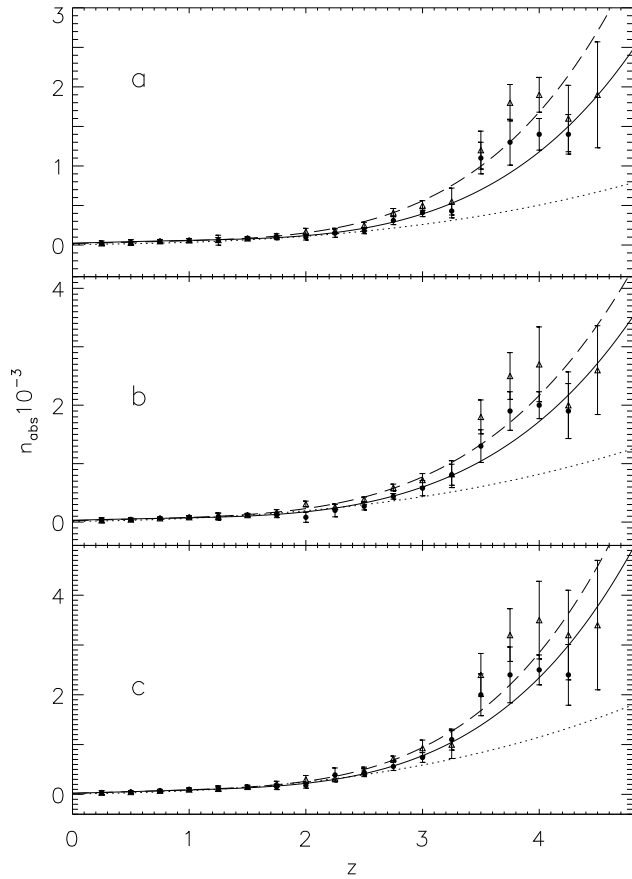


Figure 2. The redshift distribution of absorbers for samples Q_{14}^{14} (points & solid lines) and Q_{14}^{138} (triangles & long dashed lines), for cosmological models with $\Omega_m = 0.3$, $\Omega_\Lambda = 0.7$ (a), $\Omega_m = 0.5$, $\Omega_\Lambda = 0$ (b), and $\Omega_m = 1$ (d). Dot lines show the best two parameters fit for the filamentary component only at $z \leq 3$.

4.2 Redshift distribution of weaker Ly- α lines

The samples of weaker absorbers are rich enough but, even so, the main fraction of observed absorbers is concentrated near $z \sim 2.5 - 3.3$. In Figs. 3 & 4 the functions $n_{abs}(z)$ are plotted, for the samples Q_{14}^{13} , Q_{12}^{13} , and Q_{14}^{12} , Q_{12}^{12} , together with the four parameters fit (4.1). Both samples of poor absorbers with $\log N_{HI} \leq 13$ are incomplete. The best fit parameters κ_f , c_f , κ_{pan} , and c_{pan} listed in Table 4 are weakly sensitive to the used cosmological models.

These results show that, at redshifts $z \leq 1.5 - 2$, an essential fraction of weaker absorbers can be associated with the periphery of filaments and/or with possible membranes and bridges between branches of filaments, what is consistent with the expectations of Fernandes-Soto et al. (1996). But at high redshifts, the main fraction of poorer absorbers is certainly identified with the population of low mass pancakes and, for $N_{HI} \leq 10^{13} \text{ cm}^{-2}$, with absorbers formed within expanded regions. The small value of $c_{pan} \sim 0.03 - 0.05$ suggests that these absorbers were formed at $z \approx 4 - 5$. These estimates are sensitive to the distribution of absorbers at $z \geq 3$, where the observed samples are not sufficiently representative. For these populations the random overlapping of poor absorbers in the redshift space, discussed by McGill (1990) and Levshakov & Kegel (1998), formation of absorbers within "minivoids" (Zhang et al. 1998; Davé et

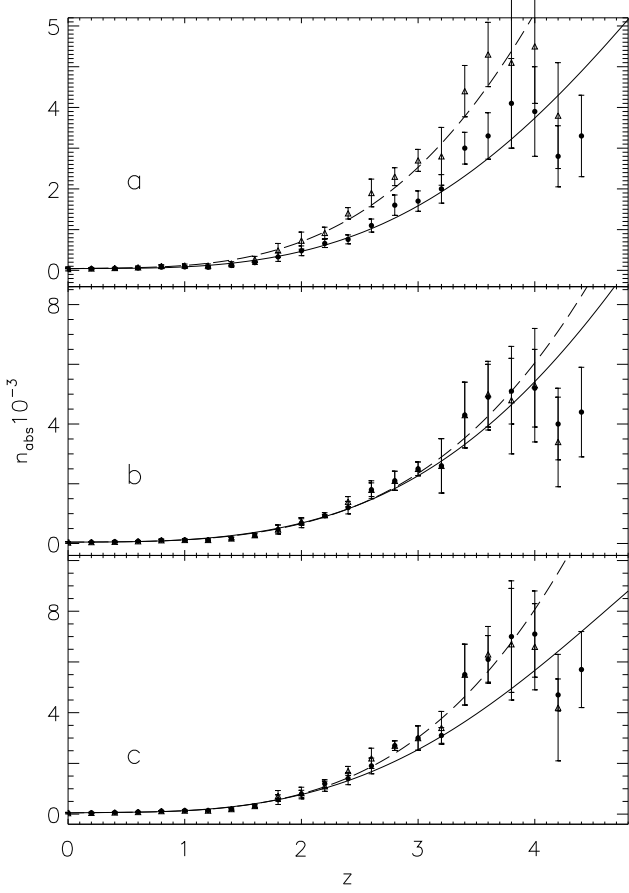


Figure 3. The redshift distribution of absorbers for the sample Q_{14}^{13} (points & solid lines) and the sample Q_{12}^{13} (triangles & long dashed lines), for cosmological models with $\Omega_m = 0.3$, $\Omega_\Lambda = 0.7$ (a), $\Omega_m = 0.5$, $\Omega_\Lambda = 0$ (b), and $\Omega_m = 1$ (c).

al. 1999) as well as the variations of UV background can distort the observed mass and temperature distribution of absorbers. As was noted in Sec. 2.1.2, at these redshifts, the more complicated three parameters function (2.11) provides better fit of observed distribution of absorbers.

The essential variations of measured linear density, n_{abs} , with respect to the smooth fitting functions are seen in Figs. 3 & 4 at $z \approx 2.5 - 3$. They can be caused, in part, by the poor statistics of absorbers, at $z \approx 2.5$, and $z \geq 3.5$. If the variations seen at $z \approx 3$ are real they can be connected with similar results obtained for the population of stronger absorbers and, thus, can indicate the period of fast transformation of pancakes into filaments. They can also be caused by influence of local factors and, first of all, by variations of background UV radiation.

The parameters of standard fit (4.3) are:

$$N_0^{pan} = 13.8 \pm 0.6, \quad \gamma_z^{pan} = 2.4 \pm 0.2, \quad \text{for } Q_{12}^{13}, \quad (4.5)$$

$$N_0^{pan} = 11.8 \pm 0.6, \quad \gamma_z^{pan} = 2.75 \pm 0.2, \quad \text{for } Q_{12}^{12}, \quad (4.6)$$

with a weak dependence on the parameters of considered cosmological models. The power index γ_z^{pan} is close to the value found earlier (see, e.g., Carswell 1995; Cristiani et al. 1996).

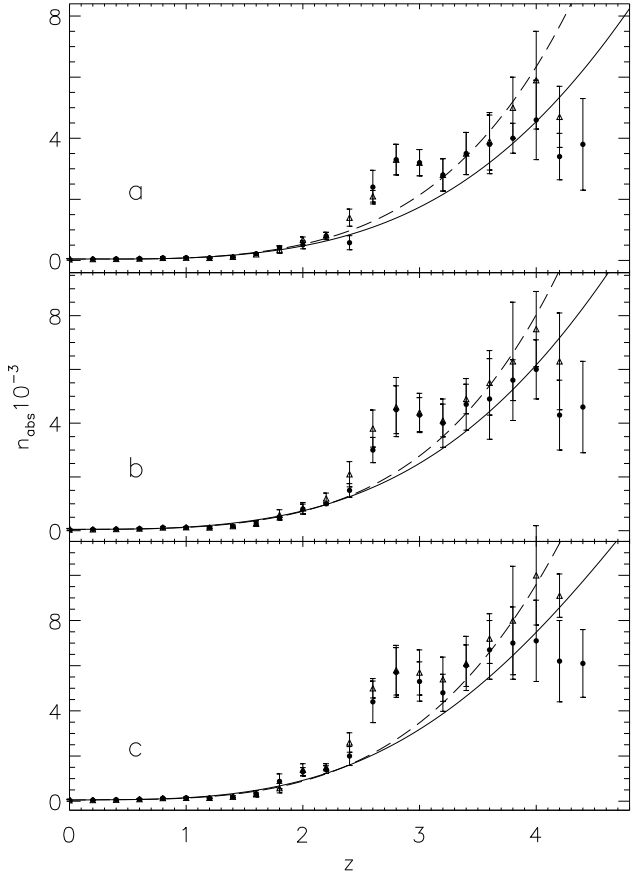


Figure 4. The redshift distribution of absorbers for the sample Q_{14}^{12} (points & solid lines) and the sample Q_{12}^{12} (triangles & long dashed lines), for cosmological models with $\Omega_m = 0.3$, $\Omega_\Lambda = 0.7$ (a), $\Omega_m = 0.5$, $\Omega_\Lambda = 0$ (b), and $\Omega_m = 1$ (c).

4.3 Redshift distribution of Ly- α lines with $b \geq 40\text{km/s}$ and $b \leq 20\text{km/s}$

The same technique can be applied to single out other subpopulations of absorbers such as subpopulations with lower Doppler parameter b , $b \leq 20\text{km/s}$, and larger, $b \geq 40\text{km/s}$. The main results of this analysis are plotted in Fig. 5, and the best fitting parameters are listed in Table 5. Unfortunately, they cannot be complemented by HST data at smaller redshifts.

These subpopulations are not so representative and at $z \leq 4$ they contain only 640 lines with $b \leq 20\text{km/s}$ and 727 lines with $b \geq 40\text{km/s}$. This is the main source of the large errors of fitting parameters listed in Table 5. Nonetheless, these results demonstrate that, if the subpopulation of hot absorbers with $b \geq 40\text{km/s}$ can be associated with pancakes, then the redshift distribution of cold absorbers with $b \leq 20\text{km/s}$ is similar to that found for filamentary component of the structure.

5 SUMMARY AND DISCUSSION.

In this paper the observed redshift distributions of Ly- α lines and metal systems are analyzed and interpreted in the framework of theoretical model of DM structure evolution (DD99). The observed evolution of absorbers depends on

Table 4. Fitting parameters of redshifts distribution of absorbers for three cosmological models.

sample	κ_f	R_{eff} $100h^{-1}\text{kpc}$	c_f	κ_{pan}
$\Omega_m = 1, \Omega_\Lambda = 0$				
Q_{14}^{14}	22 ± 1.3	2.2 ± 0.1	0.34 ± 0.14	0.75 ± 0.12
Q_{14}^{138}	21 ± 1.2	2.1 ± 0.1	0.33 ± 0.15	0.91 ± 0.11
Q_{14}^{13}	43 ± 1.5	4.3 ± 0.1	1.0 ± 0.20	4.2 ± 0.11
Q_{14}^{13}	43 ± 1.3	4.3 ± 0.1	1.0 ± 0.20	3.7 ± 0.11
Q_{12}^{12}	45 ± 1.6	4.4 ± 0.1	1.1 ± 0.22	4.8 ± 0.11
Q_{12}^{12}	49 ± 2.1	4.8 ± 0.2	1.1 ± 0.21	4.0 ± 0.09
$\Omega_m = 0.5, \Omega_\Lambda = 0$				
Q_{14}^{14}	30 ± 1.5	2.9 ± 0.2	0.66 ± 0.21	1.2 ± 0.11
Q_{14}^{138}	23 ± 1.3	2.3 ± 0.1	0.54 ± 0.22	1.6 ± 0.14
Q_{14}^{13}	39 ± 1.5	3.8 ± 0.2	1.82 ± 0.37	6.4 ± 0.12
Q_{14}^{13}	39 ± 1.4	3.8 ± 0.2	1.62 ± 0.35	5.8 ± 0.15
Q_{12}^{12}	44 ± 1.6	4.4 ± 0.6	1.93 ± 0.33	6.7 ± 0.10
Q_{12}^{12}	38 ± 2.0	3.8 ± 0.2	1.63 ± 0.42	5.6 ± 0.15
$\Omega_m = 0.3, \Omega_\Lambda = 0.7$				
Q_{14}^{14}	23 ± 1.2	2.2 ± 0.1	0.6 ± 0.16	0.8 ± 0.12
Q_{14}^{138}	18 ± 1.0	1.7 ± 0.1	0.6 ± 0.18	1.1 ± 0.11
Q_{14}^{13}	37 ± 1.8	3.6 ± 0.2	1.8 ± 0.40	4.7 ± 0.12
Q_{12}^{12}	37 ± 1.3	3.6 ± 0.1	1.1 ± 0.26	4.1 ± 0.12
Q_{14}^{12}	41 ± 1.4	4.0 ± 0.1	2.0 ± 0.33	4.4 ± 0.09
Q_{12}^{12}	42 ± 2.1	4.2 ± 0.2	2.2 ± 0.35	4.4 ± 0.11

Table 5. Fit parameters for the subsamples of absorbers Q_{14}^{12} with $b \geq 40\text{km/s}$ and $b \leq 20\text{km/s}$

Ω_m	Ω_Λ	κ_f	κ_{pan}	$10^2 \cdot c_{pan}$
$b > 40\text{km/s}$				
1.0	0	0.0	2.4 ± 2.4	5.4 ± 2.2
0.5	0	0.0	1.9 ± 2.0	3.6 ± 6.0
0.3	0.7	0.0	2.4 ± 3.1	7.7 ± 4.1
$b < 20\text{km/s}$				
1.0	0	11 ± 4.2	0.12 ± 0.1	1.0 ± 0.5
0.5	0	16 ± 10	0.0	0.0
0.3	0.7	10 ± 4.6	0.0	0.0

several random factors and does not trace directly the evolution of the DM component. Our results show however that the observed redshift distributions of absorbers can be reasonably described even by the discussed model.

The main results of our analysis can be summarized as follows:

(i) The different redshift distributions of stronger and weaker absorbers favor the existence of two distinct subpopulations of Ly- α absorbers: a rapidly evolving subpopulation of weaker absorbers, that dominates at high redshifts, and more slowly evolving subpopulation of stronger absorbers, that dominates at low redshifts (Bahcall et al. 1996). This result coincides with theoretical expectations.

(ii) The expected evolution of filamentary component of structure describes adequately the redshift distribution of metal systems, and stronger Ly- α lines, at $z \leq 3$. This strong correlation of evolutionary rate and the column density of absorbers suggests possible identification of stronger absorbers with the filamentary component of observed galaxy distribution.

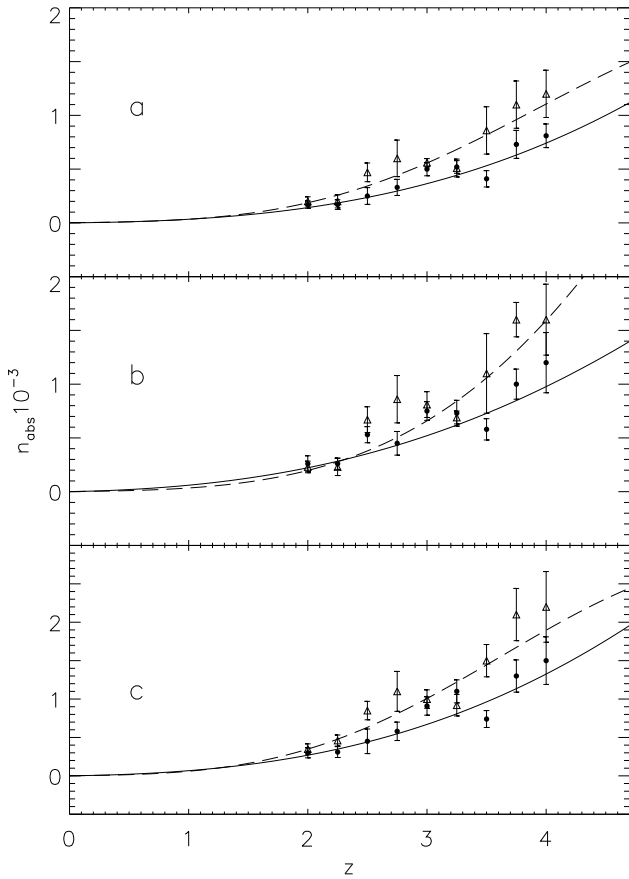


Figure 5. The redshift distribution of 640 lines with $b \leq 20\text{km/s}$, (points, solid lines), and 727 lines with $b \geq 40\text{km/s}$ for the sample Q_{14}^{12} , for three cosmological models with $\Omega_m = 0.3, \Omega_\Lambda = 0.7$, (a), $\Omega_m = 0.5, \Omega_\Lambda = 0$, (b), and $\Omega_m = 1$, (c).

(iii) The subpopulation of colder absorbers, with $b \leq 20\text{km/s}$, can be probably related with the filamentary component of the structure.

(iv) The rapid evolution of the linear number density of weaker absorbers, n_{abs} , can be naturally explained by the model of separate DM confined pancakes that are merging and expand or contract in transversal direction, as it is described by the theoretical model discussed above. At $z \leq 2 - 2.5$, disruption of the compressed matter can essentially accelerate the evolution of this subpopulation.

(v) The observed redshift distribution of absorbers depends on the influence of irregular local factors, such as variations of background UV radiation, and shock heating of gas produced by activity of galaxies. This impact is seen as irregular variations of the observed linear number density of absorbers around the smooth fitting curves.

(vi) The obtained estimates of c_f can be interpreted as a probable pick of the rate of formation of filaments at $z \sim 2 - 2.5$ whereas their enrichment by the metals can occur at $z \sim 2$ and smaller. The small values of c_{pan} , found for all subpopulations under investigation, show that the main fraction of observed poor absorbers can be associated with DM structure elements formed at redshifts $z \geq 5$.

The main quantitative characteristics of redshift distribution of absorbers, discussed above, admit natural interpretation and coincide with published estimates (see, e.g., Hu et

al. 1995; Lanzetta et al. 1995; Cristiani 1995, 1996; Le Brune 1996; Bahcall 1996). They are roughly consistent with the expected evolution of DM structure and can be, in principle, used to test and to discriminate different cosmological models. Now the best fit is obtained for the model with $\Omega_m = 0.3$, $\Omega_\Lambda = 0.7$, but the more representative database at redshifts $z \sim 2 - 2.5$ and $z \geq 3$ is required for more reliable discrimination of cosmological models.

On the other hand, the discussed rough model of structure evolution ignores many details, such as, for example, the continual variation of morphological characteristics of structure elements, and does not describe the disruption of structure. This model could be improved, but then it is inevitable to increase the number of fit parameters and, so, it will be justified only when richer sets of observed absorbers, especially at smaller and higher redshifts become available. This comment applies also to the more detailed description of expected variations of UV radiation and possible contribution of artificial caustics. Application of this approach to available simulations could test and improve it as well.

The wall-like structure elements and large under dense regions found in distribution of galaxies at small redshifts cannot yet be reliably identified with the available database. The large scale modulation of redshift distribution of Ly- α lines found by Cristiani et al. (1997) and strong nonhomogeneities, found recently at $z \leq 2$, by Williger et al. (1996), Quashnock et al. (1996, 1998), and Connolly et al. (1997) could be probably attributed to such rare extremely rich structure elements. Appearance of such elements is not forbidden at any redshifts, but it can be expected that their number will rapidly decrease for larger redshifts.

Acknowledgments

We are grateful to Dan Vanden Berk for providing the new list of observed metal systems. This paper was supported in part by Denmark's Grundforskningsfond through its support for an establishment of Theoretical Astrophysics Center, by the Polish State Committee for Scientific Research grant Nr. 2-P03D-014-17, and the grant INTAS-93-68. AGD and VIT also wish to acknowledge support from the Center of Cosmo-Particle Physics in Moscow. Furthermore, we wish to thank the anonymous referee for many useful comments.

REFERENCES

Bahcall J.N., Bergeron J., Boksenberg A. et al., 1993, *ApJS.*, **87**, 1.

Bahcall J.N., Bergeron J., Boksenberg A. et al., 1996, *ApJ.*, **457**, 19.

Bardeen J.M., Bond J.R., Kaiser N., Szalay A., 1986, *ApJ.*, **304**, 15

Bergeron J., Cristiani S., & Shaver P.A., 1992, *A&A*, **257**, 417

Bryan G.L., Machacek M., Anninos P., Norman M.L., 1999, *517*, 13

Bond J.R., Szalay A.S., & Silk J., 1988, *ApJ.*, **324**, 627

Bond J.R., & Wadsley J.W., 1997, in "Structure and Evolution of the Intergalactic Medium from QSO Absorption Line Systems", eds. P.Petitjean, S. Charlot, p. 143.

Buryak O., Demianksi M., Doroshkevich A., 1991, *ApJ.*, **383**, 41

Buryak O.E., Doroshkevich A.G., Fong R., 1994, *ApJ.*, **434**, 24

Carswell R.F., Lanzetta K.M., Parnell H.C., & Webb J.K., 1991, *ApJ.*, **371**, 36

Carswell R.F., 1995, in Meylan J., ed., QSO Absorption Lines, p. 313

Charlton J.C., 1995, in Meylan J., ed., QSO Absorption Lines, p. 405

Cole S., Weinberg D.H., Frenk C.S., & Ratra B., 1997, *MNRAS*, **289**, 37.

Cole S., Hatton, S., Weinberg D.H. & Frenk C.S., 1998, *MNRAS*, **300**, 945

Connolly A.J., Szalay A.S., Romer A.K., et al., 1996, *ApJ.*, **473**, L67

Cooke A.J., Espy B., & Carswell R., 1997, *MNRAS*, **284**, 552

Cristiani S., D'Odorico S., Fontana A., et al., 1995, *MNRAS*, **273**, 1016.

Cristiani S., D'Odorico S., D'Odorico V., et al., 1996, *MNRAS*, **285**, 209

Cowie L., Songaila A., Kim T.S., & Hu E.M., 1995, *AJ.*, **109**, 1522.

Davè R., Hernquist L., Katz N., Weinberg D., 1999, *ApJ.*, **511**, 521.

de Lapparent V., Geller M.J., Huchra J.P., 1988, *ApJ.*, **332**, 44

Demianksi M. & Doroshkevich A., 1999, *MNRAS*, **306**, 779, (DD9)

Demianksi M., Doroshkevich A., Müller V., Turchaninov V., 1999, *MNRAS*, in press, (DDMT).

Dinshaw N., Foltz C.B., Impey C.D., et al., 1995, *Nature*, **373**, 223.

Doroshkevich A., 1980, *Sov.Astron.* **24**, 152.

Doroshkevich A., Tucker, D.L., Oemler, A.A., et al., 1996, *MNRAS*, **283**, 1281. (LCRS1)

Doroshkevich A., Müller V., Retzlaff J., Turchaninov V., 1999b, *MNRAS*, **306**, 575, (DMRT)

Doroshkevich A., Fong R., McCracken G., Ratcliffe A., Shanks T., Turchaninov V., 2000, *MNRAS*, in press

Fernandes-Soto A., Lanzetta K.M., Barcon X., et al., 1996, *ApJ.*, **460**, L85.

Giallongo E., Cristiani S., Fontana A., & Trevese D., (1993), *ApJ.*, **416**, 137

Governato F., Baugh C.M., Frenk C.S., et al. 1998, *Nature*, **392**, 389.

Haardt F., Madau P., 1996, *ApJ.*, **461**, 20

Hernquist L., Katz N., Weinberg D.H., Miralda-Escude J., 1996, *ApJ.*, **457**, L51.

Hu E.M., Tae-Sun K., Cowie L., & Songaila A., 1995, *AJ*, **110**, 1526

Hui L., Gnedin N.Y., & Zhang Yu., 1997, *ApJ*, **486**, 599.

Ikeuchi S., Ostriker J.P., 1986, *ApJ.*, **301**, 522.

Jannuzi B.T., et al., 1998, *ApJS*, **118**, 976

Jenkins A., Frenk C.S., Pearce F.R. et al., 1998, *ApJ.*, **499**, 20.

Khare P., Srianand R., York D.G., et al., 1997, *MNRAS*, **285**, 167.

Kim T.S., Hu E.M., Cowie L.L., & Songaila A., 1997, *AJ*, **114**, 1.

Kirkman D., & Tytler D., 1997, *ApJ.*, **484**, 672.

Kendall M., & Moran P., 1963, *Geometrical Probability*, (London: Griffin)

Kulkarni V.P., Huang K., Green R., et al., 1996, *MNRAS*, **279**, 197

Lanzetta K.M., Bowen D.V., Tytler D., & Webb J.K., 1995, *ApJ.*, **442**, 538.

Le Brune V., Bergeron J., & Boisse P., 1996, *A&A*, **306**, 691

Levshakov S.A., Kegel W.H., 1996, *MNRAS*, **278**, 497.

Levshakov S.A., Kegel W.H., 1997, *MNRAS*, **288**, 787.

Lu L., Sargent W.L.W., Womble D.S., Takada-Hidai M., 1996, *ApJ.*, **472**, 509

McGill C., 1990, *MNRAS*, **242**, 544

Machacek M., Bryan G.L., Meiksin A., Anninos P. et al. 2000, *ApJ.*, **532**, 118

Meiksin A., 1998, in 'Eighteenth Texas Symposium on Relativistic Astrophysics and Cosmology' "Texas in Chicago", eds. A.V.Olinto, J.A.Frieman & D.Schramm, World Scientific, p. 661.

Miralda-Escude J., Rees M.J., 1993, MNRAS, **260**, 616.

Miralda-Escude J., Cen R., Ostriker J.P., & Rauch M., 1996, ApJ., **471**, 582.

Morris S.L., Weymann R.J., Dressler A., et al., 1993, ApJ., **419**, 524.

Nath B.B., 1997, ApJ., **482**, 621.

Petitjean P., Mücket J.P., & Kates R.E., 1995, A&A, **295**, 9.

Petitjean P., 1997, in The evolution of the universe, ed. G.Börner & S.Gottlöber, John Wiley & sons, Chichester, p. 261

Quashnock J.M., Vanden Berk D.E., York D.G., 1996, ApJ., **472**, L69

Quashnock J.M., Vanden Berk D.E., York D.G., 1998, in 'Eighteenth Texas Symposium on Relativistic Astrophysics and Cosmology' "Texas in Chicago", eds. A.V.Olinto, J.A.Frieman & D.Schramm, World Scientific, p. 655.

Ramella M., Geller M.J., Huchra J.P., 1992, ApJ., **384**, 396

Ratcliffe, A., Shanks, T., Broadbent, A., et al., 1996, MNRAS, **281**, L47.

Rauch M., Carswell R.F., Webb J.K., & Weymann R.J., 1993, MNRAS, 260, 589.

Rees M.J., 1986, MNRAS, **218**, 25p.

Rees M.J., 1995, in Meylan J., ed., QSO Absorption Lines, p. 419.

Rodriguez-Pascual P.M., de la Fuente A., 1995, ApJ., **448**, 575.

Sargent, W.L.W., Young, P.J., Boksenberg, A. & Tytler, D., 1980, Ap.J.Suppl., **42**, 41

Shandarin S., Zel'dovich Ya.B., 1989, Rev.Mod.Phys., **61**, 185

Shandarin S., Melotte A.L., McDavitt K., Pauls J.L., Tinker J., 1995, Phys.Rev.Let., **75**, 7

Shectman S.A., Landy S.D., Oemler A., et al., 1996, ApJ., **470**, 172.

Shull J.M., 1997, in "Structure and evolution of the intergalactic medium from QSO absorption line systems", ed. P.Petitjean, S.Charlot, p 101

Theuns T., Leonard A., Efstathiou G., Pearce E.R., Thomas P.A., 1998, MNRAS, **301**, 478

Theuns T., Leonard A., Schaye J., Efstathiou G., 1999, MNRAS, **303**, 58

Tytler D., 1995, in Meylan J., ed., QSO Absorption Lines, p. 289.

Ulmer A., 1996, ApJ., **473**, 110.

Valageas P., Schaeffer R., Silk J., 1999, AA, **345**, 691

Valinia A., Shapiro, P.R., Martel H., & Vishniac E.T., 1997 ApJ., **479**, 46.

Vanden Berk D.E., et al., 1999, ApJS., in press.

Vishniac E.T., 1983, ApJ., **274**, 152.

Weinberg D. et al., 1998, in "Evolution of Large Scale Structure: From Recombination to Garching", eds. A.J. Banday, R.K. Sheth, L.N. Da Costa, p. 346

Weymann R.J., Jannuzzi B.T., Lu L., et al., 1998, ApJ., **506**, 1

Williger G.M., Baldwin J.A., Carswell R.F. et al., 1994, ApJ., **428**, 574

Williger G.M., Hazard C., Baldwin J.A., & McMahon R.G., 1996, ApJS., **104**, 145.

Zhang Yu., Anninos P., Norman M.L., 1995, ApJ., **453**, L57

Zhang Yu., Anninos P., Norman M.L., Meiksin A., 1997, ApJ., **485**, 496

Zhang Yu., Meiksin A., Anninos P., Norman M.L., 1998, ApJ., **495**, 63

Zel'dovich, Ya.B., Novikov, I.D., 1983, The Structure and Evolution of the Universe, University of Chicago Press, Chicago.

Zel'dovich Ya.B., 1970, A&A, **5**, 20